New [M(R,R′timdt)$_2$] Metal-Dithiolenes and Related Compounds (M = Ni, Pd, Pt; R,R′timdt = Monoanion of Disubstituted Imidazolidine-2,4,5-trithiones): An Experimental and Theoretical Investigation

Maria Carla Aragoni,[†] Massimiliano Arca,[†] Francesco Demartin,[‡] Francesco A. Devillanova,*,[†] Alessandra Garau,[†] Francesco Isaia,[†] Francesco Lelj,[§] Vito Lippolis,[†] and Gaetano Verani[†]

Contribution from the Dipartimento di Chimica e Tecnologie Inorganiche e Metallorganiche, Università di Cagliari, Via Ospedale 72, 09124 Cagliari, Italy, Dipartimento di Chimica Strutturale e Stereochimica Inorganica e Centro CNR, Università di Milano, Via G. Venezian 21, 20133 Milano, Italy, and Dipartimento di Chimica, Università della Basilicata, Via N. Sauro 85, 85100 Potenza, Italy

Received March 15, 1999

Abstract: Several new Ni (**7a**−**i**), Pd (**8a**−**j**), and Pt (**9a**−**j**) dithiolenes belonging to the general class [M(R,R′timdt)$_2$] (R,R′timdt = monoanion of di-substituted imidazolidine-2,4,5-trithione) have been synthesized by sulfuring the disubstituted imidazolidine-2-thione-4,5-diones (**4**) with Lawesson's reagent (**5**) in the presence of the appropriate metal either as powder or as chloride. The obtained compounds have been characterized by UV−vis−NIR, FT-IR, and FT-Raman spectroscopies, CP-MAS ^{13}C NMR, and cyclic voltammetry, while [Ni(Me,Pr^{i}timdt)$_2$] (**7c**) was also characterized by X-ray diffraction on a single crystal. Isolation from the reaction mixtures of the complex *trans*-bis[*O*-ethyl(4-methoxyphenyl)phosphonodithioato]Ni(II) (**10a**) and of 4,5,6,7-tetrathiocino[1,2-*b*:3,4-*b*′]diimidazolyl-1,10-diphenyl-3,8-diethyl-2,9-dithione (**6a**) as byproducts supports a radical mechanism for the one-pot reaction leading to the title dithiolenes. All these complexes absorb in the NIR region in the range 991−1030 nm with extinction coefficients of rarely encountered magnitudes (up to 80000 M^{-1} cm^{-1}). They are therefore ideal candidates for applications on Nd:YAG laser technology for which the excitation wavelength is 1064 nm. Hybrid-DFT calculations have been used to gain an insight on the properties of this class of dithiolenes compared with those of the simplest [M(S$_2$C$_2$H$_2$)$_2$] [M = Ni (**1**); M = Pd (**2**); M = Pt (**3**)] and of the well-known [M(dmit)$_2$] [dmit = C$_3$S$_5^{2-}$, 1,3-dithiole-2-thione-4,5-dithiolate; M = Ni (**11**); M = Pd (**12**); M = Pt (**13**)] dithiolenes.

Introduction

Metal−dithiolenes represent a very important class of coordination compounds because of their unique properties, such as intense vis−NIR absorption, electrical conduction,[1,2] and optical nonlinearity[3] and the ability to exist in several clearly defined oxidation states connected through fully reversible redox steps.[4] The best known dithiolenes are certainly those derived from the dmit ligand (dmit = C$_3$S$_5^{2-}$, 1,3-dithiole-2-thione-4,5-dithiolate) with d^8 transition-metal ions[5] because of their interesting electrical conduction properties. At present, several superconductors deriving from the dmit ligand, such as TTF-[Ni(dmit)$_2$],[6] α-TTF[Pd(dmit)$_2$],[7] NMe$_4$[Ni(dmit)$_2$],[8] and α-[EDT-TTF][Ni(dmit)$_2$][9] (TTF = tetrathiafulvalene; EDT-TTF = ethylenedithiotetrathiafulvalene) are known.

Mueller-Westerhoff and Drexhage first reported that some neutral [Ni(S$_2$C$_2$R,R′)$_2$] dithiolenes could be used as Q-switching dyes for NIR-lasers because of their high photochemical stability

† Università di Cagliari.
‡ Università di Milano.
§ Università della Basilicata.

(1) (a) Ferraro, J. R.; Williams, J. M. *Introduction to Synthetic Electrical Conductors*; Academic: New York, 1987. (b) Nakamura, T.; Underhill, A. E.; Coomber, A. T.; Friend, R. H.; Tajima, H.; Kobayashi, A.; Kobayashi, H. *Inorg. Chem.* **1995**, *34*, 870.

(2) (a) Bousseau, M.; Valade, L.; Legros, J.-P.; Cassoux, P.; Garbauskas, M.; Interrante, L. V. *J. Am. Chem. Soc.* **1986**, *108*, 1908. (b) Kobayashi, A.; Kim, H.; Sasaki, Y.; Murata, K.; Kato, R.; Kobayashi, H. *J. Chem. Soc., Faraday Trans.* **1990**, *86*, 361.

(3) Oliver, S. N.; Kershaw, S. V.; Underhill, A. E.; Hill, C. A. S.; Charlton, A. *Nonlinear Optics* **1995**, *10*, 87.

(4) Williams, R.; Billig, E.; Waters, J. H.; Gray, H. B. *J. Am. Chem. Soc.* **1966**, *88*, 43.

(5) (a) Steimecke, G.; Sieler, H. J.; Kirmse, R.; Hoyer, E. *Phosphorus Sulfur* **1979**, *7*, 49. (b) Cassoux, P.; Valade, L.; Kobayashi, H.; Kobayashi, A.; Clark, R. A.; Underhill, A. E. *Coord. Chem. Rev.* **1991**, *110*, 115. (c) Sun, S.; Wu, P.; Zhu, D.; Ma, Z.; Shi, N. *Inorg. Chim. Acta* **1998**, *268*, 103. (d) Sato, A.; Kobayashi, H.; Naito, T.; Sakai, F.; Kobayashi, A. *Inorg. Chem.* **1997**, *36*, 5262. (e) Kochurani; Singh, H. B.; Jasinski, J. P.; Paight, E. P.; Butcher, R. J. *Polyhedron* **1997**, *16*, 3505. (f) Matsubayashi, G.; Natsuaki, K.; Nakano, M.; Tamura, H.; Arakow, R. *Inorg. Chim. Acta* **1997**, *262*, 103. (g) Yeldhuizen, Y.; Veldman, N.; Lakin, M. T.; Spek, A. L.; Paulus, P. M.; Faulmann, C.; Haasnoot, J. G.; Maaskant, M. J. A.; Reedijk, J. *Inorg. Chim. Acta* **1996**, *245*, 27. (h) Valade, L.; Legros, J.-P.; Bousseau, M.; Cassoux, P.; Garbauskas, M.; Interrante, L. V. *J. Chem. Soc., Dalton Trans.* **1985**, 783. (i) Pomaréde, B.; Garreau, B.; Malfant, I.; Valade, L.; Cassoux, P.; Legros, J.-P.; Audouard, A.; Brossard, L.; Ulmet, J. P.; Doublet, M. L.; Canadell, E. *Inorg. Chem.* **1994**, *33*, 3401. (j) Fujiwara, H.; Arai, E.; Kobayashi, H. *J. Chem. Soc., Chem. Commun.* **1997**, 837.

(6) Brossard, L.; Ribault, M.; Valade, L.; Cassoux, P. *Physica B* **1986**, *143*, 378.

(7) Brossard, L.; Hurdequint, L.; Ribault, M.; Valade, L.; Legros, J.-P.; Cassaux, P. *Synth. Met.* **1988**, *27*, B157.

(8) Kobayashi, A.; Kim, H.; Sasaki, Y.; Kobayashi, H.; Moriyama, S.; Nisho, Y.; Kajita, K.; Sasaki, W. *Chem. Lett.* **1987**, 1819.

(9) Tajima, H.; Inokuchi, M.; Kobayashi, A.; Ohta, T.; Kato, R.; Kobayashi, H.; Kuroda, H. *Chem. Lett.* **1993**, 1235.

10.1021/ja990827x CCC: $18.00
Published on Web 07/20/1999

Table 1. Main Spectral Properties and Redox Potentials for **7a−i**, **8a−j**, and **9a−j**

	M	R	R′	Raman (cm^{-1}) ν_1	Raman (cm^{-1}) ν_2	FIR (cm^{-1}) ν_1	FIR (cm^{-1}) ν_2	NIR[a] (nm)	CV (V vs F_c^+/F_c)[f] $E^{II}_{1/2}$	CV $E^{I}_{1/2}$	CV E^{III}_{pa}
7a	Ni	Me	Me	326	436[c]	432s	376m	991	−1.067(6)	−0.631(4)	+0.207
7b	Ni	Et	Et	327	435[b]	435s	378m	996	−1.095(6)	−0.650(4)	+0.233
7c	Ni	Me	Pr^i	335	434[b,c]	436s	381m	996	−1.093(4)	−0.640(2)	+0.273
7d	Ni	Me	*n*-Pentyl	326	433[b,d]	437s	376m	997	−1.070(2)	−0.634(3)	+0.228
7e	Ni	Et	*n*-Pentyl	327	433[d]	434s	378m	998	−1.14(2)	−0.660(3)	+0.363
7f	Ni	Me	*n*-Nonyl	335	433[d]	435s	377m	996	−1.093(3)	−0.648(3)	+0.273
7g	Ni	Et	Ph	332	435[b,d]	436s	380m	1010	−1.062(1)	−0.584(6)	+0.298
7h	Ni	Me	*p*-ClPh	330	*d*	436s	376m	1008	−0.963[e]	−0.513[e]	+0.218
7i	Ni	Me	*p*-CH_3OPh	331	*d*	434s	381m	1009	−0.948[e]	−0.503[e]	
8a	Pd	Me	Me	340	429[b]	419s		1010			
8b	Pd	Et	Et	341	430[b]	428s	392m	1010	−0.960(4)	−0.596(3)	+0.238[g]
8c	Pd	Me	Pr^i	348	427[b]	431s		1013	−0.952(7)	−0.600(3)	+0.203[g]
8d	Pd	Me	*n*-Pentyl	341	429[b]	431s		1017	−0.956(8)	−0.594(6)	+0.208
8e	Pd	Et	*n*-Pentyl	341	429[b,c]	430s		1019	−0.961(6)	−0.601(2)	+0.208[g]
8f	Pd	Me	*n*-Nonyl	340	430[b]	429s	392mw	1020	−0.942(1)	−0.591(2)	+0.223[g]
8g	Pd	Et	Ph	342	430[b]	429s		1030	−0.910(3)	−0.547(2)	+0.343
8h	Pd	Me	*p*-ClPh	341	429[d]	431s		1030	−0.833[e]	−0.468[e]	+0.243
8i	Pd	Me	*p*-CH_3OPh	342	425[d]	428s		1030	−0.873[e]	−0.523[e]	+0.287
8j	Pd	Me	*p*-NO_2Ph	343	433[d]	427s		1030			
9a	Pt	Me	Me	375	*c*	421s, 425 sh		993	−0.968[e]	−0.543[e]	
9b	Pt	Et	Et	375	*b,c*	428s	390m	998	−1.056(4)	−0.614(4)	+0.342[e]
9c	Pt	Me	Pr^i	383	*b,c*	421s, 425s		997	−1.059(7)	−0.613(1)	+0.338[e]
9d	Pt	Me	*n*-Pentyl	376	423[c]	426s		999	−1.053(7)	−0.606(2)	+0.368[g]
9e	Pt	Et	*n*-Pentyl	376	422[b,c]	426s		1004	−1.060(8)	−0.619(2)	+0.363[g]
9f	Pt	Me	*n*-Nonyl	377	*c*	420s		1001	−1.054(1)	−0.609(2)	+0.343[e]
9g	Pt	Et	Ph	378	*c*	427s		1012	−1.016[e]	−0.565(2)	+0.318[e]
9h	Pt	Me	*p*-ClPh	377	*c*	431s		1010	−0.924[e]	−0.479[e]	
9i	Pt	Me	*p*-CH_3OPh	377	*c*	427s		1010			
9j	Pt	Me	*p*-NO_2Ph	378	*c*	426s		1010	−0.919[e]	−0.474[e]	+0.397[e]

[a] Molar extinction coefficient $\epsilon > 60000$ M^{-1} cm^{-1} for all compounds. [b] Raman spectra recorded in $CHCl_3$ solution, laser power 200 mW, 200 scans. [c] Raman spectra recorded as KBr pellet, 300 mW, 200 scans. [d] Raman spectra recorded on the solid compound, 350 mW, 200 scans. [e] Anodic peak recorded at scan rate of 100 mV s^{-1}. [f] CV recorded at scan rates varying between 50 and 1000 mV s^{-1} (in parenteses are sd's calculated on values obtained at different scan rates). Potential values are referred to $E_{1/2}$ of the reversible F_c^+/F_c couple. Solubility problems did not allow to record the voltammograms for compounds **8a**, **8j**, and **9i**. [g] Quasi-reversible process.

and intense vis−NIR absorption.[10] This absorption, attributed to a $\pi-\pi^*$ electronic transition[11] between the HOMO and the LUMO, occurs at energy values depending on the nature of the R and R′ substituents. For the simplest dithiolenes (R = R′ = H, often reported as "parent dithiolenes") this absorption was observed at 720, 785, and 680 nm for [Ni($S_2C_2H_2$)$_2$][12] (**1**), [Pd($S_2C_2H_2$)$_2$] (**2**), and [Pt($S_2C_2H_2$)$_2$] (**3**), respectively.[13] It has been shown that when R and R′ act as donors, the vis−NIR absorption occurs at lower energies.[14]

Recently, some new neutral [Ni(R_2timdt)$_2$] complexes [R = Et (**7b**), Pr^i (**7k**), Bu (**7l**); R_2timdt = monoanion of dialkylimidazolidine-2,4,5-trithione], differing from the dithiolenes derived from the dmit ligand in that they have NR groups instead of *endo*cyclic sulfurs, have been reported.[15−17] These complexes are characterized by an absorption at about 1000 nm of rarely encountered intensity ($\epsilon \approx 80000$ M^{-1} cm^{-1} for **7k**) compared to those of similar compounds. The more recently reported [Pd(Et$_2$timdt)$_2$] (**8b**)[18] shows the NIR absorption band at 1010 nm with a molar extinction coefficient of 70000 M^{-1} cm^{-1}. The wavelength and the high intensity of the NIR absorption band also propose this new class of dithiolenes as candidates for Q-switching the Nd:YAG laser (excitation wavelength 1064 nm).

To obtain dithiolenes characterized by the NIR absorption as close as possible to the excitation wavelength of the Nd:YAG laser, we have systematically varied either the central metal or the substituents R and R′ in the [M(R,R'timdt)$_2$] dithiolene unit. Therefore, dithiolenes with M = Ni (**7a−i**), Pd (**8a−j**), and Pt (**9a−j**) have been synthesized, starting from 10 different imidazolidine-2-thione-4,5-diones (**4a−j**) (see Table 1 and Scheme 1). The properties of the synthesized dithiolenes have been deeply explored using FT-IR, FT-Raman, CP-MAS ^{13}C NMR, and UV−vis−NIR spectroscopies and cyclic voltammetry. To understand the physical−chemical properties of these new compounds on the basis of their electronic structures, we have performed Hybrid-DFT[19] calculations on the unsubstituted [M(H_2timdt)$_2$] complexes [M = Ni (**14**), Pd (**15**), Pt (**16**)], on the [M($S_2C_2H_2$)$_2$] parent dithiolenes [M = Ni (**1**), Pd (**2**), Pt

(10) (a) Drexhage, K. H.; Mueller-Westerhoff, U. T. *IEEE Quantum Electron* **1972**, QE-8, 759. (b) Drexhage, K. H.; Mueller-Westerhoff, U. T. US Patent 3743964, 1973.

(11) Mueller-Westerhoff, U. T.; Vance, B.; Yoon, D. I. *Tetrahedron* **1991**, *47*, 909.

(12) Schrauzer, G. N.; Mayweg, V. P. *J. Am. Chem. Soc.* **1965**, *87*, 3585.

(13) Browall, K. W.; Interrante, L. V. *J. Coord. Chem.* **1973**, *3*, 27.

(14) (a) Mueller-Westerhoff, U. T.; Vance, B. *Comprehensive Coordination Chemistry*; Pergamon Press: New York, 1987; Vol. 2, Chapter 16.5, p 595. (b) Yoon, D. I. Ph.D. Thesis, University of Connecticut, 1988.

(15) Bigoli, F.; Deplano, P.; Devillanova, F. A.; Lippolis, V.; Lukes, P. J.; Mercuri, M. L.; Pellinghelli, M. A.; Trogu, E. F. *J. Chem. Soc., Chem. Commun.* **1995**, 371.

(16) Bigoli, F.; Deplano, P.; Devillanova, F. A.; Ferraro, J. R.; Lippolis, V.; Lukes, P. J.; Mercuri, M. L.; Pellinghelli, M. A.; Trogu, E. F. *Inorg. Chem.* **1997**, *36*, 1218.

(17) Bigoli, F.; Deplano, P.; Mercuri, M. L.; Pellinghelli, M. A.; Pintus, G.; Trogu, E. F.; Zonnedda, G.; Wang, H. H.; Williams, J. M. *Inorg. Chim. Acta* **1998**, *273*, 175.

(18) Arca, M.; Demartin, F.; Devillanova, F. A.; Garau, A.; Isaia, F.; Lelj, F.; Lippolis V.; Pedraglio, S.; Verani, G. *J. Chem. Soc., Dalton Trans* **1998**, 3731.

(19) (a) Kryachko, E. S.; Ludeña, E. V. *Energy Density Function Theory of Many Electron Systems*; Kluver Academic Publisher: Dordrect, 1990; NL. (b) Hohenberg, P.; Kohn, W. *Phys. Rev.* **1964**, *136*, 864. (c) Kohn, W.; Sham, L. J. *Phys. Rev.* **1965**, *140*, A1133. (c) Miehlich, B.; Savin, A.; Stoll, H.; Preuss, H. *Chem. Phys. Lett.* **1989**, *157*, 200. (d) Becke, A. D. *J. Chem. Phys.* **1993**, *98*, 1372.

Scheme 1. Overall Reaction Path in the Synthesis of [M(R,R′timdt)$_2$] Dithiolenes

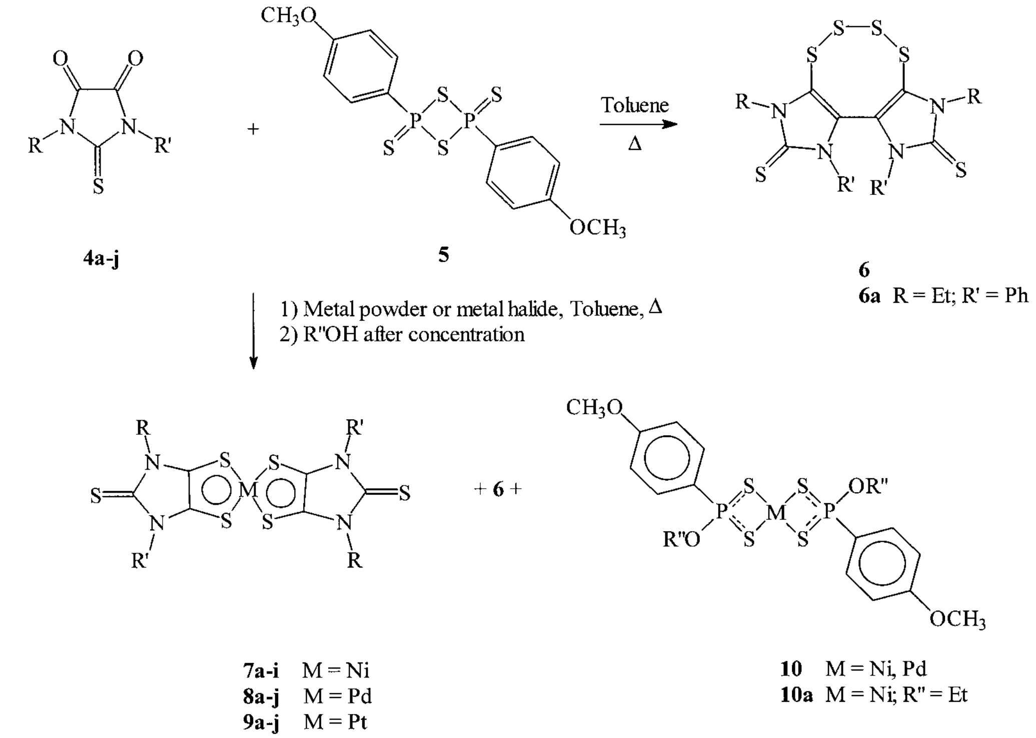

(**3**)], and on the neutral [M(dmit)$_2$] [M = Ni (**11**), Pd (**12**), Pt (**13**)] complexes that are closely related compounds, since they have S atoms instead of NR groups in their penta-atomic ring. In addition, we report the crystal structures of [Ni(Me,Pr^{i}timdt)$_2$] (**7c**), the first unsymmetrically substituted metal−dithiolene belonging to this class, and of 4,5,6,7-tetrathiocino[1,2-*b*:3,4-*b*′]diimidazolyl-1,10-diphenyl-3,8-diethyl-2,9-dithione (**6a**), which is the first unsymmetrical derivative belonging to the class of compounds **6**.[20]

Results and Discussion

The main routes for the synthesis of metal-dithiolenes consist of the reaction of either an appropriate disubstituted 1,2-dithiolate[5a,i] with a transition-metal ion or of the corresponding 1,2-dithione with the metal in its elemental state.[14a] Unfortunately, both methods are inapplicable for the syntheses of R,R′timdt-dithiolenes.[18,21] However, the direct sulfuration of the appropriate imidazolidine-2-thione-4,5-diones (**4**) with Lawesson's reagent[22] (**5**) in the presence of the metal as a powder or a halide (Scheme 1) produces the desired metal-dithiolene. While Ni complexes **7** can be obtained in fairly good yields using Ni powder, the Pd- and Pt-dithiolenes **8** and **9** require $PdCl_2$[18] and $PtCl_2$, respectively.

Although dithiolenes with unsymmetrically disubstituted ligands are not uncommon,[11] crystal structure determinations are rare, the only example being the *trans*-bis(4-*n*-octylphenyl)-nickel-dithiolene.[23] Among the present [M(R,R′timdt)$_2$] dithiolenes, only crystals of **7c** (R = Me, R′ = Pr^i) were suitable for X-ray structure determination, and they showed a trans arrangement of the ligands in the complex (Figure 1). In fact,

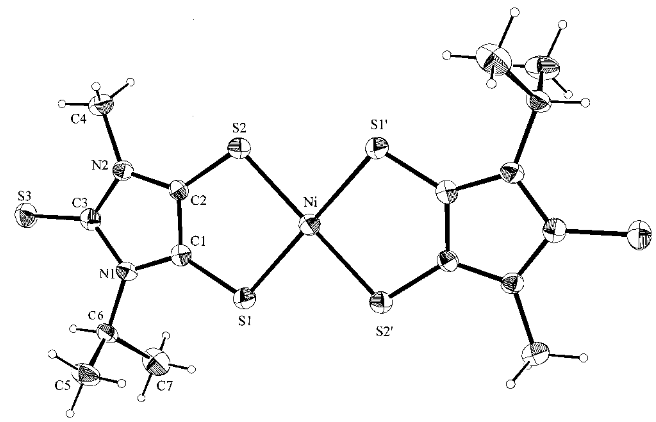

Figure 1. Molecular structure and atom labeling scheme for **7c**. Some selected interatomic distances (Å) and angles (deg) follow: Ni−S(1) 2.160(1), Ni−S(2) 2.166(1), S(1)−C(1) 1.682(5), S(2)−C(2) 1.681(5), C(1)−C(2) 1.396(6), S(1)−Ni−S(2) 94.33(5), Ni−S(1)−C(1) 101.2(2), Ni−S(2)−C(2) 100.6(2), S(1)−C(1)−C(2) 121.3(4), S(2)−C(2)−C(1) 122.5(4) and S(1)−Ni−S(2)′ 85.67(5).

the complex molecule is located about a crystallographic inversion center, and it is completely planar except for the isopropyl substituents, which are almost perpendicular to the molecular plane, with the Ni atom 0.04 Å out of plane. Bond distances and angles in the ligand are analogous to those observed for other previously characterized dithiolenes in this class.[16,18] The complex molecules are packed in the crystal, stacked parallel about along [−110], without short metal−metal interactions. The nickel atoms are sandwiched between the imidazolidine rings of molecules belonging to adjacent parallel layers, with a metal−ring (centroid) distance of 3.98 Å (Figure 2). This feature has already been observed in the crystal structure of **8b**.

The synthesis of **7**, **8**, or **9** is generally accompanied by the formation of compound **6**,[20] which becomes the main product in absence of the metal (Scheme 1). In the sulfuration reactions

(20) Atzei, D.; Bigoli, F.; Deplano, P.; Pellinghelli, M. A.; Trogu, E. F. *Phosporus Sulfur* **1988**, *37*, 189.
(21) Roesky, H. W.; Hofman, H.; Clegg, W.; Noltemeyer, M.; Sheldrick, G. M. *Inorg. Chem.* **1982**, *21*, 3798.
(22) Sheibe, S.; Pedersen, B. J.; Lawesson, S.-O. *Bull. Soc. Chim. Belg.* **1978**, *87*, 229.
(23) Cotrait, M.; Gaultier, J.; Polycarpe, C.; Giroud, A. M.; Mueller-Westerhoff, U. T. *Acta Crystallogr., Sect. C* **1983**, *39*, 833.

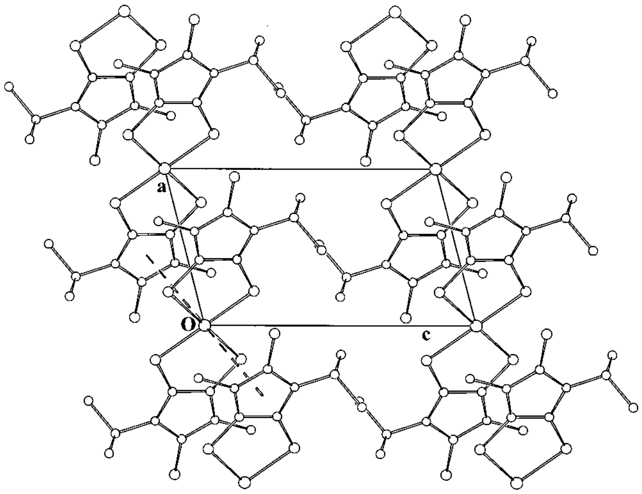

Figure 2. Crystal packing of **7c** seen along [010].

of 1,2-diones, the formation of a dithiete species in equilibrium with its dithioketonic form has been postulated[11] on the basis of the isolation of the $(CF_3)_2C_2S_2$ dithiete.[24,25] In our case, by hypothesizing an analogous equilibrium between the disubstituted imidazolidine-2,4,5-trithione and its cyclic dithiete form, the formation of **6** through the homolytic breaking of one of the two C−S bonds is easily explained. On the other hand, the formation of the symmetrical 4,5,9,10-tetrathiocino[1,2-*b*:5,6-*b*′]diimidazolyl-1,3,6,8-tetraalkyl-2,7-dithione, observed in the case of the isopropyl substituent,[16] can be explained by the homolytic breaking of either the S−S or the C−S bonds. Starting from unsymmetrical imidazolidines (**4c**−**j**), three different geometrical isomers of **6** could be expected, two (depicted in Scheme 1) belonging to the C_2, the other to the C_1 point groups depending on the position of the R and R′ groups. However, the isolation of only one of the C_2 isomers in the case of **6a** (R = Et; R′ = Ph)[26−28] should indicate that, at least in this case, the breaking of the C−S bond next to the phenyl group is preferred.

In addition, in the synthesis of the Ni- and Pd-dithiolenes, but not in the case of Pt-dithiolenes, another byproduct, i.e., bis-[*O*-alkyl-(4-methoxyphenyl)phosphonodithioato]metal complex **10** (Scheme 1),[29] which becomes the main product in absence of **4**, was identified. It is formed by opening of the P_2S_2 tetra-atomic ring of Lawesson's reagent[22] in the presence of a nucleophilic agent, which is the alcohol added to isolate the dithiolene (see Scheme 1 and Experimental Section).[29] Formation of **6** and **10** lowers the yield in dithiolene.

Vis−NIR Spectroscopy. While in the parent $[M(S_2C_2H_2)_2]$ dithiolenes the characteristic $\pi-\pi^*$ transition falls at 720, 785, and 680 nm for M = Ni (**1**), Pd (**2**), and Pt (**3**) respectively,[13] in [M(R,R'timdt)$_2$] dithiolenes it falls at ca.1000 nm (Table 1). Except for aromatic substituents, which increase the wavelength of the absorption by ∼10−15 nm, only slight shifts are observed on changing R and R′. The energy is not even modified by the introduction of substituents with different electronic effects (**4i**, **4h**, **4j**) in the para position of the phenyl group. As far as the change in the metal is concerned, the energies of the NIR absorptions for [Ni(R,R′timdt)$_2$] and [Pt(R,R′timdt)$_2$] are very similar, while for Pd-dithiolenes a slight bathochromic shift is observed (Figure 4 for **7b**, **8b**, and **9b**). As a consequence, Pd-dithiolenes with aromatic substituents (**8g**−**j**) exhibit the lowest energy absorption among the synthesized dithiolenes (1030 nm). Compared with the other known dithiolenes, the value of the molar extinction coefficient of the $\pi-\pi^*$ transition for this class of compounds is indeed surprising, since it reaches as much as 80000 M^{-1} cm^{-1}.

Vibrational Spectroscopy. The IR spectra of the dithiolenes **7a**−**i**, **8a**−**j**, and **9a**−**j** in the 3500−500 cm^{-1} region are characterized by bands deriving from the organic frameworks of the ligands, the spectra of the corresponding Ni-, Pd-, and Pt-dithiolenes being practically superimposable. More interesting is the far-IR region, where the metal−sulfur vibrations fall. The MS_4 fragment[30] (disposed on the *xy* plane) originates four stretching and four bending modes whose symmetry representations depend on the ligands. In fact, parent, dmit, and symmetrically substituted R_2timdt dithiolenes belong to the D_{2h} point group ($\Gamma_{stretching} = a_g + b_{1g} + b_{2u} + b_{3u}$; $\Gamma_{bending} = 2b_{1g} + b_{3u} + b_{2u}$), while those derived from R,R′timdt ligands belong to

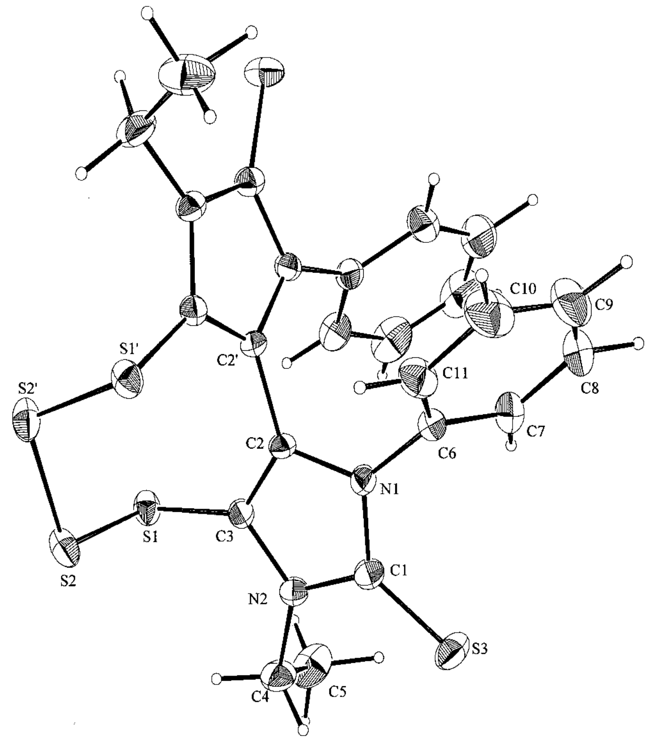

Figure 3. Molecular structure and atom labeling scheme for **6a.** Some selected interatomic distances (Å) and angles (deg) follow: N(1)−C(2) 1.401(2), C(2)−C(3) 1.356(2), C(3)−N(2) 1.400(2), N(2)−C(1) 1.367(2), C(1)−N(1) 1.377(2), C(2)−C(2)′ 1.456(3), C(3)−S(1) 1.747(2), S(1)−S(2) 2.084(1), S(2)−S(2)′ 2.043(1), S(3)−C(1) 1.678(2), C(2)′−C(2)−C(3) 129.3(1), C(2)−C(3)−S(1) 128.0(1), C(3)−S(1)−S(2) 101.42(6), S(1)−S(2)−S(2)′ 105.62(3), N(1)−C(1)−S(3) 127.5(1), S(3)−C(1)−N(2) 127.0(1).

(24) Krespan, C. G. *J. Am. Chem. Soc.* **1961**, *83*, 3434.

(25) Davison, A.; Edelstein, E.; Holm, R. H.; Maki, A. H. *Inorg. Chem.* **1964**, *3*, 814.

(26) A picture of **6a** is displayed in Figure 3. Crystallographic data are reported in the Experimental Section. The molecule is located about a crystallographic 2-fold axis, passing through the midpoint of the C2−C2′ and S2−S2′ bonds. The two imidazole rings are twisted 72° about the C2−C2′ bond. Such a conformation is assumed in order to minimize the tensions within the octa-atomic ring and does not seem to be due to the hindrance of the phenyl groups. In fact, similar torsion values have been found in the 4,5,6,7-tetrathiocino[1,2-*b*:3,4-*b*′]diimidazolyl-1,3,8,10-tetraethyl-2,9-dithione (70°) and in its 1:2 adduct with molecular di-iodine (76°).[Ref.s 20,27] In **6a**, phenyl groups show a parallel orientation analogous to the one found in the tetraphenyl derivative.[28]

(27) Atzei, D.; Bigoli, F.; Deplano, P.; Pellinghelli, M. A.; Sabatini, A.; Trogu, E. F.; Vacca, A. *Can. J. Chem.* **1989**, *67*, 1416.

(28) Mercuri, M. L. *Tesi di Dottorato in Scienze Chimiche*, Cagliari, Italy, 1993.

(29) Arca, M.; Cornia, A.; Devillanova, F. A.; Fabretti, A. C.; Isaia, F.; Lippolis, V.; Verani, G. *Inorg. Chim. Acta* **1997**, *262*, 81.

(30) Schläpfer, C. W.; Nakamoto, K. *Inorg. Chem.* **1975**, *14*, 6.

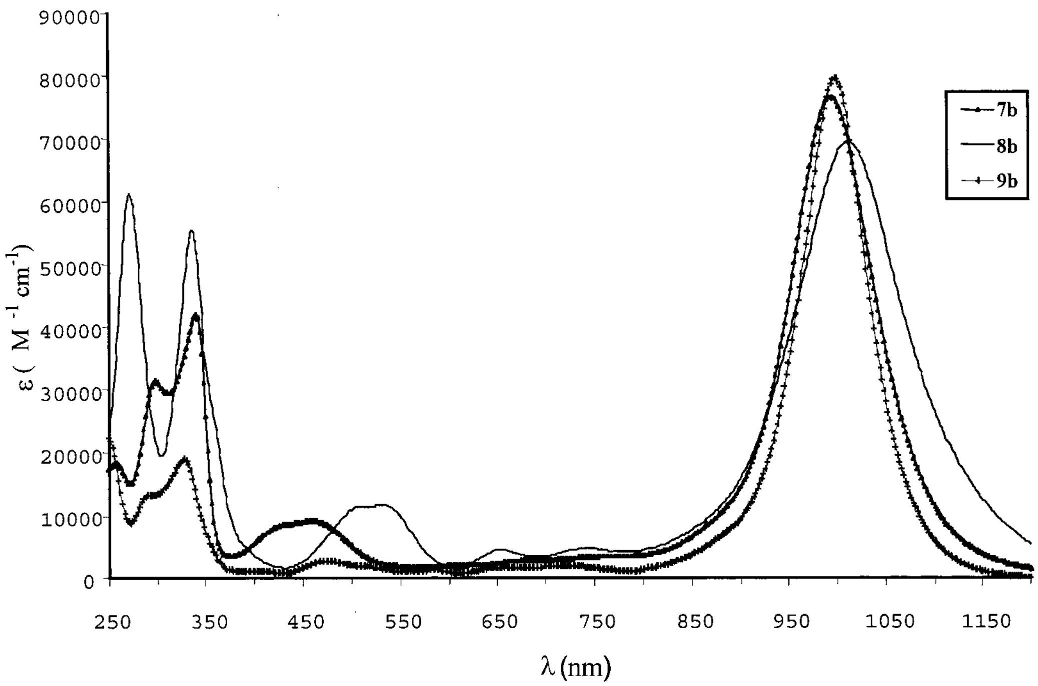

Figure 4. UV−vis−NIR spectra of **7b**, **8b**, and **9b** in $CHCl_3$ solutions.

C_{2h} ($\Gamma_{stretching} = 2a_g + 2b_u$; $\Gamma_{bending} = 2a_g + 2b_u$) or C_{2v} ($\Gamma_{stretching} = 2a_1 + 2b_2$; $\Gamma_{bending} = 2a_1 + 2b_2$) point groups, depending on their composition and coordination modes (trans or cis, respectively). The far-IR spectra show two bands, whose frequencies are almost unaffected by R and R′ and slightly depend on the metal (Table 1). The most intense band is found at 435(2), 427(3), and 425(3) cm^{-1} (average values) for **7a**−**i**, **8a**−**j**, and **9a**−**j**, respectively. The second band falls at average values of 380(2) and 339(2) cm^{-1} for **7a**−**i** and **8a**−**j**, respectively, while it is not visible in the FIR spectra of **9a**−**j**.

Because of the resonance Raman effect, Raman spectra show only two very intense peaks in the 500−50 cm^{-1} region, falling at average wavenumbers of 330(4) and 434(1) cm^{-1} for **7a**−**i**, 342(2) and 429(2) cm^{-1} for **8a**−**j**, and 377(3) and 422(1) cm^{-1} for **9a**−**j**, showing that they only depend on the metal.

Since R and R′ do not affect the vibrational spectra in the low region, no information can be derived on the symmetries of dithiolenes having R ≠ R′. However, on the basis of the mutual exclusion rule between Raman and IR bands, the trans arrangement (C_{2h}) found in **7c** should be extended to all unsymmetrical dithiolenes.

CP-MAS ^{13}C NMR Spectroscopy. All the signals of the carbon atoms in [M(R,R′timdt)$_2$] dithiolenes fall in the expected region, and only small variations in the chemical shifts of the carbons of the dithiolene framework are observed on changing the substituents R and R′, the average values being 163(1), 164.9(6), and 165(2) ppm for Ni-, Pd-, and Pt-dithiolenes, respectively. More interestingly, these peaks are often doubled also when R = R′. The spectrum of **7c** shows a difference of about 2.5 ppm in the chemical shifts of C(1) and C(2). Correspondingly, the N(2)−C(2) and N(1)−C(1) bonds differ by 0.015 Å. Splittings of 1.9 and 1.6 ppm have been observed, for example, for [Pd(Me$_2$timdt)$_2$] and [Pt(Me$_2$timdt)$_2$], respectively. In these cases, the splittings should be determined by an asymmetry induced by the packing effects.

Cyclic Voltammetry. Half-wave potentials for the synthesized compounds are reported in Table 1. The voltammograms of Ni-dithiolenes show two reversible monoelectronic reductions ($E^{\mathrm{I}}_{1/2}$ and $E^{\mathrm{II}}_{1/2}$) and one bielectronic oxidation ($E^{\mathrm{III}}_{\mathrm{pa}}$), which is

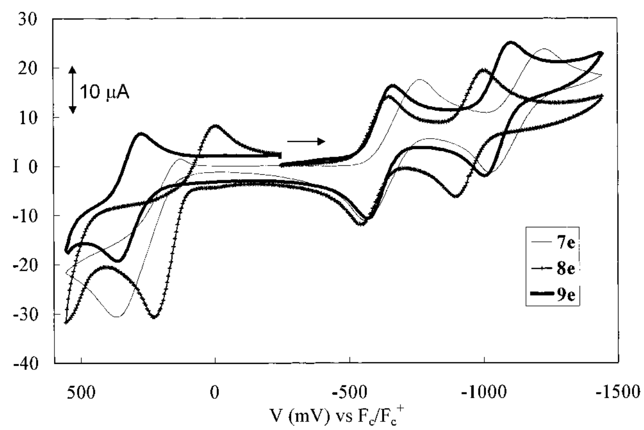

Figure 5. CV curves for **7e**, **8e**, and **9e** recorded at a platinum electrode on an anhydrous methylene chloride solution (supporting electrolyte TBAFA 5 × 10^{-2} M; scan rate 0.100 V s^{-1}).

irreversible for Ni-dithiolenes and quasi-reversible in the case of Pd- and, in some instances, Pt-dithiolenes. The voltammograms of **7e**, **8e**, and **9e** are superimposed in Figure 5 . The oxidation probably only regards the coordinated ligands, as previously found in the mixed-valence compound obtained by reacting [Ni(Pr$^i_2$timdt)$_2$] (**7k**) and an excess of I_2.[16] The reduction potentials of Pd-derivatives, particularly $E^{\mathrm{II}}_{1/2}$, related to the process [M(R,R′timdt)$_2$]$^-$/[M(R,R′timdt)$_2$]$^{2-}$ (Table 1), are generally less negative than those of Ni- and Pt-dithiolenes, which are very close to each other.[31]

For Ni- and Pt-dmit derivatives, the [M(dmit)$_2$]/[M(dmit)$_2$]$^-$ process is irreversible and is observed at +0.22 and +0.19 V vs Ag/AgCl, respectively, in MeCN, while the reversible reduction to the bianionic form is found at −0.13 V vs Ag/AgCl for both complexes.[32] In the case of [Pd(dmit)$_2$], the CV in MeCN is similar to that measured for [Ni(dmit)$_2$], but the

(31) The averaged potentials are −1.09(3), −0.95(2), and −1.056(3) V vs F_c^+/F_c [−0.45(3), −0.30(2) and −0.409(3) V vs Ag/AgCl 3.5 M] for **7a**−**i**, **8b**−**i** and **9a**−**j**, respectively.

(32) Kato, R.; Kobayashi, H.; Kobayashi, A.; Yukiyoshi, S. *Bull. Chem. Soc. Jpn.* **1986**, *59*, 627.

anodic peaks merge.[5i] At any rate, the higher potentials of the dmit dithiolenes compared to those measured for our complexes account for the higher stability of the neutral form of the $[M(R,R'timdt)_2]$ complexes. The oxidation process is absent in the dmit complexes, but it has often been observed in other metal-dithiolenes, such as $[Ni(ddds)_2]$ and $[Ni(dddt)_2]$ (E_{pa} = +0.71 and +0.99 V respectively vs Ag/AgCl in PhCN; ddds = 5,6-dihydro-1,4-dithiin-2,3-diselenolate, $C_4H_4S_2Se_2$; dddt = 5,6-dihydro-1,4-dithiin-2,3-dithiolate, $C_4H_4S_4$).[5j] Also the parent-dithiolenes show values of the first reduction potentials (+0.11, +0.17 and +0.10 V in MeCN solution vs Ag/AgCl for **1**, **2** and **3** respectively)[13] higher than those of our $[M(R,R'timdt)_2]$ dithiolenes ($E^{I}_{1/2}$ in Table 1). Accordingly, their monoreduced forms are more stable than the neutral ones.

Hybrid-DFT Calculations. To understand the differences in the properties of the $[M(R,R'timdt)_2]$ dithiolenes compared to those of the parent compounds (**1**−**3**) and of the neutral $[M(dmit)_2]$ (**11**−**13**), we carried out DFT calculations[19] on the three series of compounds, since this type of calculation gives encouraging results with inorganic compounds containing transition metals[33] in their ground or excited states.[34] Although the Shafer et al. VDZ basis set[35] has been previously used for **14**,[18] the Hay-Wadt LANL2DZ basis sets[36] together with ECP sets have now been employed to extend the calculations to the heavier Pd and Pt atoms. In consideration of the fact that the R and R′ substituents have very little influence on the previously discussed properties, the calculations have been carried out on the model $[M(H_2timdt)_2]$ [M = Ni (**14**), Pd (**15**), Pt (**16**)] complexes. As a confirmation of this, a more complex calculation was performed on **7a**, obtaining results very similar to those calculated for **14** as regards optimized structural parameters, Kohn−Sham orbital energies, and charge distribution. For all calculations, *inter*molecular interactions, such as π-interactions leading to dimer formation and dimer−monomer and dimer−dimer contacts, have been neglected, although they can be relevant for dmit and parent dithiolenes.[5−9,11,14,38] A comparison between calculated and experimental structural parameters (crystal structures have only been reported for **1**−**3**,[37,38] **7c**, **7k**,[16] **8b**,[18] and **11**[5h]) shows that metal−sulfur distances are generally overestimated by about 0.05 Å in the calculations, while *intra*ligand distances and angles are in very good agreement. For all compounds, the ground configuration belongs to the A_{1g} representation. In Figure 6, sketches of HOMOs and LUMOs for Ni-dithiolenes **1**, **11**, and **14** are reported. The b_{1u} HOMO (numbered as 55 for **1**−**3**, 107 for **11**−**13**, and 91 for **14**−**16** according to a progressive labeling based on an energy scale) is a m.o. mainly made up of the four $3p_z$ a.o.'s of the sulfur donor atoms, perpendicular to the molecular *xy* plane and the four $2p_z$ carbon a.o.'s taken with opposite phases. In the dmit and H_2timdt derivatives, also the *endo*cyclic S and N ring atoms (for **11**−**13** and **14**−**16**, respectively) and to a higher extent the terminal sulfurs participate in this m.o. In each case, the very low contribution of the $(n + 1)p_z$ a.o.'s of the metal decreases on passing from Ni to Pd and Pt (n = 3, 4, 5 for Ni, Pd, and Pt, respectively). The 56/92/108 b_{2g} π^*-LUMO is fully delocalized on the whole molecule except the nitrogen and sulfur ring atoms (for **14**−**16** and **11**−**13**, respectively) and involves

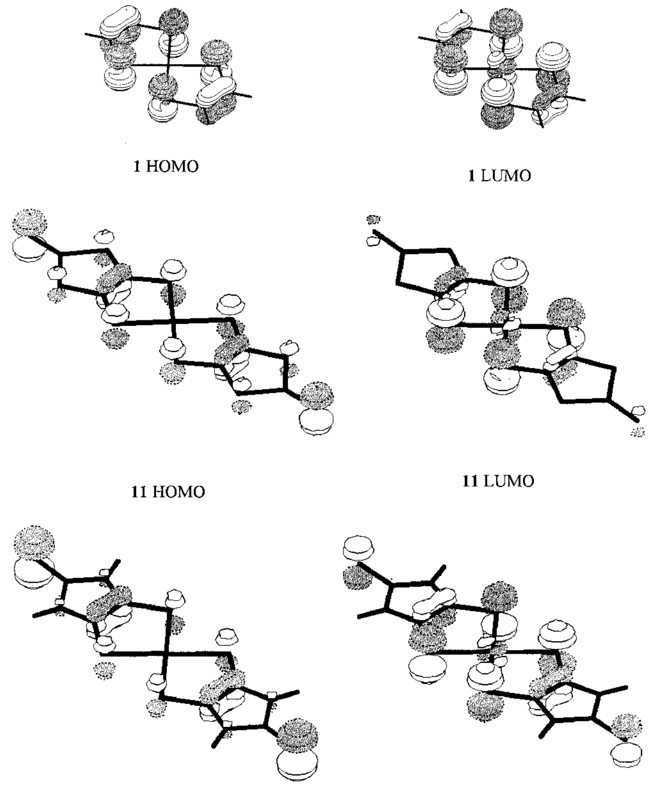

Figure 6. Sketches of HOMOs and LUMOs for **1, 11** and **14**.

directly the metal atom through its nd_{xz} a.o.'s, with increasing contribution on passing from Ni to Pd and Pt. A correlation diagram between the corresponding orbitals of the three classes of dithiolenes is shown in Figure 7. For **11**−**13** and **14**−**16**, the additional m.o.'s arising from the H_2timdt and the dmit ligands modify the energies of the b_{1u} HOMO and b_{2g} LUMO orbitals. As a consequence, the energy gap ΔE between these two orbitals significantly decreases on passing from **1**−**3** to **11**−**13** and to **14**−**16** (Table 2). A similar consideration might be invoked to explain the effect of aromatic substituents in $[M(R,R'timdt)_2]$ dithiolenes: additional low-lying π orbitals able to interact with the HOMO should contribute to raise its energy by further lowering the $\pi-\pi^*$ energy gap. The observed trend confirms previous EHT results,[39] which predict that donor substituents induce a bathochromic shift in the lowest energy transition.

Since Koopman's theorem does not apply to DFT, the energies of Kohn−Sham orbitals cannot be used as in the case of Hartree−Fock calculations; nevertheless the energy difference ΔE between the HOMO and the LUMO can be considered a valuable parameter. Therefore, this may be related to the energy of the intense NIR transition, which varies from about 14000 cm^{-1} for **1**−**3** to about 10000 cm^{-1} for the complexes deriving from the R,R′timdt ligand, while for **11**−**13** no experimental electronic spectra have been reported so far. In Figure 8, the calculated ΔE values are reported versus the experimental energies of the lower energy transition. Since the correlation is very good, we reckon it should be possible to estimate the wavelengths of the electronic absorption for **11**−**13** (900, 950, and 890 nm, respectively).

It must be noted that DFT calculations carried out on the dmit complexes have already been reported.[40] However, they

(33) Adamo, C.; Lelj, F. *J. Chem. Phys.* **1995**, *103*, 10605.
(34) Daul, C. *Int. J. Quantum Chem.* **1994**, *52*, 867.
(35) Schafer, A.; Horn, H.; Ahlrichs, R. *J. Chem. Phys.* **1992**, *97*, 2571.
(36) (a) Hay, P. J.; Wadt, W. R. *J. Chem. Phys.* **1985**, *82*, 270. (b) Dunning, T. H., Jr.; Hay, P. J. In *Methods of Electronic Structure Theory*; Schaefer, H. F., III, Ed.; Plenum Press: New York, 1977; Vol. 2.
(37) Eisenberg, R. *Prog. Inorg. Chem.* **1970**, *12*, 295.
(38) Browall, K. W.; Bursh, T.; Interrante, L. V.; Kasper, J. S. *Inorg. Chem.* **1972**, *11*, 8.
(39) Nazzal, A.; Lane, R. W.; Mayerle, J. J.; Mueller-Westerhoof, U. T. Final Report USARO, United States NTIS **1978**, *78*, 137.
(40) Rosa, A.; Riccardi, G.; Baerends, E. J. *Inorg. Chem.* **1998**, *37*, 1368.

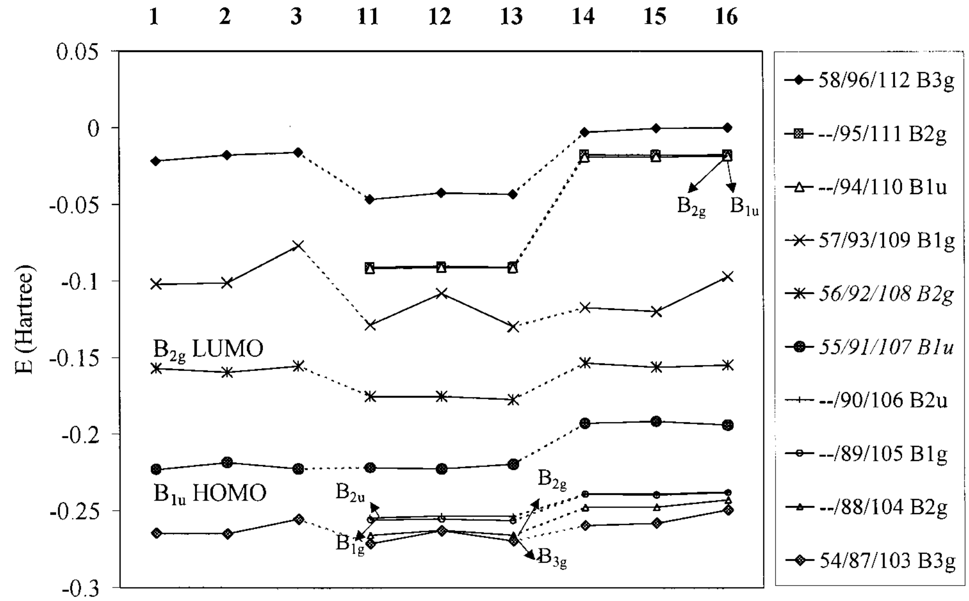

Figure 7. Calculated orbital energies (Hartree) of the frontier orbitals in **1**−**3**, **11**−**13**, and **14**−**16**. The box shows the representations of m.o.'s in the D_{2h} point group together with their labelings.

Table 2. Calculated[a] and Experimental $\pi-\pi^*$ Transition Energies (E, cm^{-1}) and Wavelengths (λ, nm) for 1−3, 11−13 and 14−16

	E		λ	
	calcd	exptl	calcd	exptl
1	14512	13900	689	720
2	12919	12740	774	785
3	14740	14720	678	680
11	10190		981	
12	9247		1081	
13	10381		963	
14[b,c]	8705	10000	1149	1000
15[b]	7807	9700	1281	1015
16[b]	8601	10000	1163	1000

[a] pVDZ Basis set by Schafer, Horn, and Ahlrichs[35] for C, H, N, S atoms; Hay and Wadt LANL2DZ Basis set with ECP[36] used for the metal atoms. [b] The experimental values reported for compounds **14**−**16** have been averaged on **7a**−**i**, **8a**−**j**, and **9a**−**j**, respectively. [c] Calculated and experimental energies and wavelengths for **7a** are 8599, 10091 cm^{-1} and 1163, 991 nm.

were performed using the experimental data from the structures of TTF[Ni(dmit)$_2$]$_2$,[2a] Me$_4$N[Pd(dmit)$_2$]$_2$,[41] and TTF[Pt(dmit)$_2$]$_3$[2a] without optimization of the geometries. Moreover, a different functional was used, and no HF non-local exchange corrections were introduced, as in the case of the Becke3LYP functional. Furthermore, Slater-type orbitals and frozen-core approximations were used. As a consequence, while the atomic orbital contributions to HOMO and LUMO are similar in both calculations, the order of the molecular orbitals lying below the HOMO as well as the HOMO−LUMO energy gap ΔE values (0.76, 0.61, and 0.62 eV[40] compared with 1.27, 1.83, and 1.30 eV for **11**−**13**, respectively) are different.

As expected, in **14**−**16** the LUMO energies follow the same trend as the reduction potentials measured for **7a**−**i**, **8a**−**j**, and **9a**−**j** (see Figure 9 for **7b**, **8b**, and **9b**), although the changes in the thermodynamic parameters involved in the redox process leading to charged species are neglected. The comparison of the LUMO's energies of the three series of compounds shows that [M(dmit)$_2$] complexes are much more easily reducible and, therefore, their anionic forms are more stable than the neutral ones, as observed experimentally. On the contrary, the reductions of **14**−**16** to anionic species are more difficult, since their LUMO energies are the highest among the examined complexes.

(41) Kobayashi, A.; Hyerjoo, K.; Sasaki, Y.; Murata, K.; Kato, R.; Kobayashi, H. *J. Chem. Soc., Faraday Trans.* **1990**, *86*, 361.

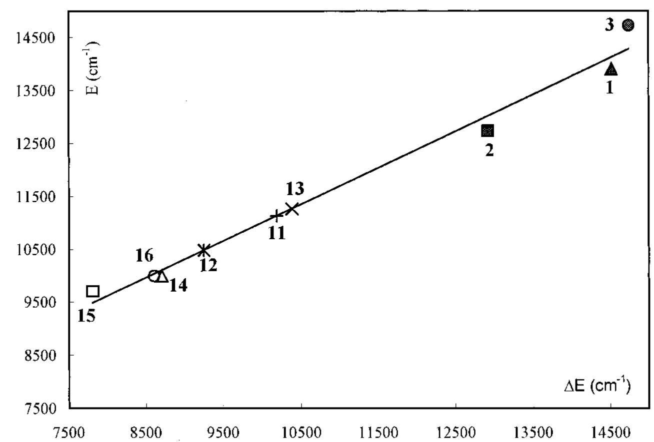

Figure 8. Calculated ΔE values for **1**−**3** and **14**−**16** vs experimental vis-NIR transitions for **1**−**3** and **14**−**16** (the values for **14**−**16** have been averaged on **7a**−**i**, **8a**−**j**, and **9a**−**j**, respectively). Using the ΔE values calculated for **11**−**13**, it might be possible to evaluate their approximate electronic absorptions (900, 950, and 890 nm, respectively).

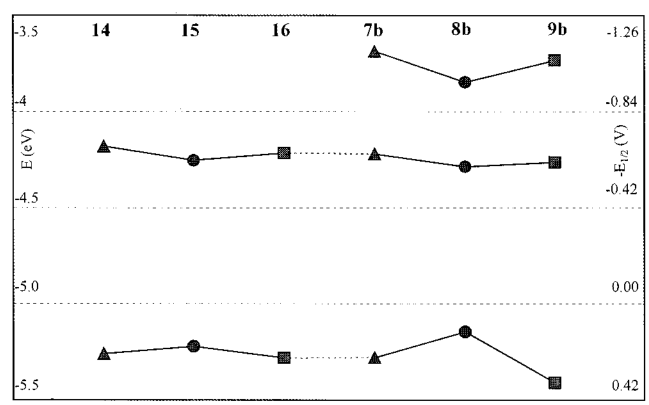

Figure 9. HOMO and LUMO energies (calculated for **14**−**16**) compared with experimental halfwave potentials vs F_c^+/F_c for **7b** (triangles), **8b** (circles), and **9b** (squares). E_{pa} values are reported for the oxidation process.

Table 3. Calculated[a] Mulliken Charges (e) for **1**−**3**, **11**−**13**, **14**−**16** (Atom Numbering as in Figure 1)

compd	M	S(1,2)	C(1,2)	X(1,2)[b]	C(3)	S(3)
1	−0.060[c]	−0.014	−0.028			
2	−0.186	0.022	−0.031			
3	−0.247	0.029	−0.021			
11	−0.005	−0.008	−0.094	0.233	−0.205	−0.053
12	−0.142	0.036	−0.103	0.231	−0.204	−0.053
13	−0.206	0.045	−0.093	0.230	−0.203	−0.053
14[d]	−0.013	−0.060	0.056	−0.072	0.074	−0.196
15	−0.154	−0.019	0.043	−0.071	0.074	−0.196
16	−0.233	−0.008	0.058	−0.074	0.074	−0.202

[a] pVDZ Basis set by Schafer, Horn, and Ahlrichs[35] for C, H, N, S atoms; Hay and Wadt LANL2DZ basis set with ECP[36] used for the metal atoms. [b] X = S for **11**−**13**; X = N for **14**−**16**. [c] The Mulliken charge calculated on the Ni atom using a simpler HF method was −0.070 e. See: Fischer-Hjalmars, I.; Henriksson-Enflo, A. *Int. J. Quantum Chem.* **1980**, *18*, 409. [d] The Mulliken charges calculated for **7a** are −0.003, −0.084, 0.070, −0.221, 0.115, and −0.222 e.

The calculated energies of the HOMOs of the three series explain the differences in oxidation processes, which are achievable only in our dithiolenes (see the Cyclic Voltammetry section). Moreover, since the HOMO does not involve the metal orbitals, it is not surprising that the change of the metal does not affect the oxidation potentials. This agrees with the structural features of the only oxidized dithiolene in this series isolated so far, which shows that the oxidation is ligand-centered.[16]

The calculated Mulliken charges[42] (Table 3) show that in all series the metal becomes remarkably more negative on passing from Ni to Pd and Pt, while the charges on the sulfur donor atoms tend to become less negative or neutral. The charges on the N−C(=S)−N and S−C(=S)−S groups of H_2timdt and dmit ligands are unaffected by the change in the metal. Accordingly, the chemical shift of the C(3) carbon (Mulliken charge +0.074 e) is very similar in **7a**−**i**, **8a**−**j**, and **9a**−**j**.

Finally, the DFT calculations help understand the nature and type of the vibrational bands observed with FT-IR and FT-Raman techniques in the far-IR region (500−50 cm^{-1}; Table 4). In **1**−**3**, almost pure normal modes are found, and the assignments based on DFT-calculations only partially agree with the previously published[43,44] normal coordinate analyses, which were not complete in the far-IR region, and led to conflicting assignments. As far as the dmit derivatives are concerned, despite the large amount of publications regarding their properties, only a few spectroscopic studies have been reported.[45] Recently,[46] the Raman-active a_g bands have been identified on the basis of their depolarization ratios in **11** and [Pd(dmit)$_2$]$^{-0.5}$(**17**), since [Pd(dmit)$_2$] had never been isolated. The calculated frequencies of the a_g modes (134, 341, 368, 499, 500, 962, 1122, 1385 cm^{-1} and 119, 340, 365, 494, 503, 945, 1121, 1384 cm^{-1} for **11** and **12**, respectively) are in good agreement with those found in the experimental Raman spectra of **11** and **17** (140, 343, 364, 488, 496, 950, 1051, 1399 cm^{-1} and 140, 345, 364, 485, 515, 1078, 1354 cm^{-1}). These assignments are similar to those proposed by Ramakumar et al.[47] on the basis of ab initio calculations.[48]

Coming to our dithiolenes, the most intense band, originated from a b_{3u} bending mode, falls at 434, 429, and 431 cm^{-1} for **14**, **15**, and **16**, respectively. These values are in very good agreement with the experimental bands found at average values of 435(2), 427(3), and 425(3) cm^{-1} for **7a**−**i**, **8a**−**j**, and **9a**−**j**, respectively. The calculated b_{2u} stretching mode is expected to be not very intense and to fall at 380, 334, and 319 cm^{-1} in **14**, **15**, and **16**, respectively. As seen in the Vibrational Spectroscopy section, this band appears as a medium band at an average value of 380(2) cm^{-1} for [Ni(R,R′timdt)$_2$] and as a very weak band at 339(2) cm^{-1} for [Pd(R,R′timdt)$_2$], but it is not visible in Pt complexes. As regards the Raman peaks, DFT calculations predict the a_g stretching mode at 312, 325, and 353 cm^{-1} in **14**, **15**, and **16** in quite good agreement with the average experimental values found for **7a**−**i**, **8a**−**j**, and **9a**−**j** [330(4), 342(2), and 377(3) cm^{-1}, respectively].[49] This is the most intense band, since it is resonance enhanced (excitation energy of the Nd:YAG laser 1064 cm^{-1}).[16] The shift toward higher energies on passing from Ni to Pt had already been observed in [M(mnt)$_2$]$^{2-}$ [mnt = maleonitriledithiolate;[50] $\nu(a_g)$ = 335, 349, 378 cm^{-1} for M = Ni, Pd, and Pt, respectively] and was attributed to an increased metal-*d*/ligand-π orbital overlap.[51] The second Raman peak falling at average values of 434(1), 429(2), and 422(1) cm^{-1} for Ni, Pd, and Pt (only visible in **9d** and **9e**) complexes, respectively, might be attributed either to a_g or b_{1g} bending modes (calculated frequencies 444, 439, and 440 cm^{-1} and 443, 443, and 444 cm^{-1} for **14**, **15**, and **16** respectively).

Conclusions

Due to their photochemical and thermal stabilities and to their very strong absorption in the NIR region, which is close to the Nd:YAG excitation energy (1064), [Ni(R$_2$timdt)$_2$] dithiolenes have proved to be ideal candidates for Q-switching this type of laser. With the aim of getting closer to the desired wavelength, several Ni (**7a**−**i**), Pd (**8a**−**j**), and Pt (**9a**−**j**) dithiolenes belonging to the general [M(R,R′timdt)$_2$] class of compounds have been synthesized and fully characterized by means of several techniques. In the case of asymmetric ligands, vibrational spectroscopies support a trans orientation, confirmed for **7c** by an X-ray crystal structure determination. Therefore, all the considered dithiolenes belong to the centrosymmetric D_{2h} (R = R′) or C_{2h} (R ≠ R′) point groups. Electrochemical measurements demonstrate that while the oxidation of Pd-dithiolenes over the neutral state is achievable and quasi-reversible, it is irreversible both in Ni and Pt analogues. The syntheses of these

(42) In the present case, the slight difference in Ni charge magnitude (−0.013 e) compared to the previously reported value for **14** (−0.017 e[18]) depends on the change in basis set and on the use of effective core potentials.

(43) Adams, D. M.; Cornell, J. B. *J. Chem. Soc. A* **1968**, 1299.

(44) Siimann, O.; Fresco, J. *Inorg. Chem.* **1971**, *10*, 2.

(45) (a) Papavassiliou, G.; Cotsilios, A. M.; Jacobsen, C. S. *J. Mol. Struct.* **1984**, *115*, 41. (b) Tajima, H.; Naito, T.; Tamura, M.; Kobayashi, A.; Kato, R.; Kobayashi, H.; Clark, R. A.; Underhill, A. E. *Mol. Cryst. Liq. Cryst.* **1990**, *181*, 233. (c) Tajima, H.; Naito, T.; Tamura, M.; Takahashi, A.; Toyoda, S.; Kobayashi, A.; Kuroda, H.; Kato, R.; Kobayashi, H.; Clark, R. A.; Underhill, A. E. *Synth. Metals* **1991**, *41*, 2417. (d) Tamura, M.; Masuda, R.; Tajima, H.; Kuroda, H.; Kobayashi, A.; Yakushi, K.; Kato, R.; Kobayashi, H.; Tokumoto, M.; Kinoshita, N.; Anzai, H. *Synth. Metals* **1991**, *41*, 2499. (e) Underhill, A. E.; Clark, R. A.; Marsden, I. *J. Phys. Condens. Matter* **1991**, *3*, 933. (f) Jacobsen, C. S.; Yartsev, V. M.; Tanner, D. B.; Bechgaard, K. *Synth. Metals* **1993**, *55*−*57*, 1925. (g) Nakamura, T.; Underhill, A. E.; Coomber, A. T.; Friend, R. H.; Tajima, H.; Kobayashi, A.; Kobayashi, H. *Inorg. Chem.* **1995**, *34*, 870. (h) Liu, H. L.; Tanner, D. B.; Pullen, A. E.; Abboud, K. A.; Reynolds, J. R. *Phys. Rev.* **1996**, *B53*, 10557.

(46) Pokhodnya, K. I.; Faulmann, C.; Malfant, I.; Andreu-Solano, R.; Cassoux, P.; Mlayah, A.; Smirnov, D.; Leotin, J. Private comunication. The paper will be published in the *Proceedings of the International Conference on Science and Technology of Synthetic Metals*, 1998.

(47) Ramakumar, R.; Tanaka, Y.; Yamaji, K. *Phys. Rev.* **1997**, *B56*, 795.

(48) Seger, D. M.; Korzenietski, C.; Kowalchik, W. *J. Phys. Chem.* **1991**, *95*, 69.

(49) In the case of [Ni(Pr$^i{}_2$timdt)$_2$], this band (346 cm^{-1}) has similarly been attributed to the a_g totally symmetric stretching mode.[16]

(50) (a) Gray, H. B.; Billig, E. *J. Am. Chem. Soc.* **1963**, *85*, 2019. (b) Davidson, A.; Edelstein, N.; Holm, R. H.; Maki, A. H. *ibidem* **1963**, *85*, 2029; *Inorg. Chem.* **1963**, *2*, 1227.

(51) Clark, R. J. H.; Turtle, P. C. *J. Chem. Soc., Dalton Trans.* **1977**, 2142

Table 4. Calculated Vibrational Frequencies (cm^{-1}; IR Relative Intensities in Parentheses; KM mol^{-1}) and Experimental[a] Vibration Frequencies (cm^{-1}) for **1−3**, **11−13**, and **14−16**

	calculated					experimental	
	bending			stretching			
compd	b_{1u}	a_g	b_{3g}	b_{2u}	$a_g(I)$	FIR	Raman
1[a]	302 (3.6)	214		415 (4.1)	335	309m, 428m	
2[a]	289 (4.1)	194		350 (3.5)	346	279w, 335m	
3[a]	282 (2.4)	214		328 (24.9)	375	279m, 328m	
11[b]	497 (82)	500	351	433 (1.8)	341		343, 496
12[b]	492 (40)	494	352	410 (2.8)	341		345, 515
13	493 (39)	503	357	410 (2.5)	341		
14[c]	434 (248)	444	443	380 (10.1)	312	435(2)s, 380(2)m	330(4), 434(1)
15[c]	429 (272)	439	443	334 (9.2)	325	427(3)s, 339(2)vw	342(2), 429(2)
16[c]	431 (266)	440	444	319 (9.3)	353	425(3)s	377(3), 422(1)

[a] Reference 13. [b] Reference 46. [c] The experimental values reported for compounds **14−16** have been averaged on **7a−i**, **8a−j**, and **9a−j**, respectively.

dithiolenes by sulfuration with Lawesson's reagent[22] (**5**) of the disubstituted imidazolidine-2-thione-4,5-diones (**4**), generally occur in low yields, since they are always accompanied by the formation of several byproducts, among which bis[*O*-alkyl(4-methoxyphenyl)phosphonodithioate] complexes (**10**) and 4,5,6,7-tetrathiocino[1,2-*b*:3,4-*b*′]diimidazolyl-1,10-diphenyl-3,8-diethyl-2,9-dithione (**6a**) have been characterized by X-ray diffraction. The high yield observed in the preparation of the **6a** supports an intermediate dithiete in solution; compounds **6** should be formed by homolytic breaking of one of the C−S bonds of the dithiete. The experimental NIR features of **7a−i**, **8a−j**, and **9a−j** show that Pd complexes absorb at energies slightly lower than Ni and Pt isologues and that aromatic substituents cause an additional bathochromic shift. Thus, the Pd complexes are particularly well-suited for Q-switching applications on the Nd:YAG laser.

Experimental Section

Procedures and Methods. All solvents and reagents were Aldrich products used as purchased. All operations were carried out under dry nitrogen atmosphere. The degree of purity of each compound has been checked by CHNS and TLC analysis. The reactions involved are summarized in Scheme 1. The naming scheme according to the substituents is reported in Table 1. Elemental analyses were performed on a FISONS EA-1108 CHNS-O instrument. Infrared spectra were recorded on a Bruker IFS55 spectrometer at room temperature, purging the sample cell with a flow of dried air. Polythene pellets with a Mylar beam-splitter and polythene windows (500−50 cm^{-1}, resolution 2 cm^{-1}) and KBr pellets with a KBr beam-splitter and KBr windows (4000−400 cm^{-1}, resolution 4 cm^{-1}) were used. FT-Raman spectra were recorded with a resolution of 4 cm^{-1} on a Bruker RFS100 FT-Raman spectrometer, fitted with an In−Ga−As detector (room temperature) operating with a Nd:YAG laser (excitation wavelength 1064 nm), with a 180° scattering geometry. An appreciable decomposition of the solid compounds under laser exposure was observed. At any rate, if the sample is diluted in a KBr matrix or in $CHCl_3$ solution, no decomposition is observed. No difference in the position of the strongest bands was observed when both methods were employable, though weak bands are not clearly distinguishable on solid-state spectra. Electronic spectra were recorded with a cell of 1 cm optical path, on a Varian Cary 5 spectrophotometer in $CHCl_3$ solution at 20 °C in a thermostated compartment. ^1H NMR spectra were recorded on a Varian FT-NMR VXR 300 spectrometer operating at a frequency of 300 MHz on $CDCl_3$ solution at 20 °C. Chemical shifts were computed using TMS as an internal reference. For multiplets the mean values are reported. CP-MAS ^{13}C NMR spectra were recorded on a Varian Unity Inova 400 MHz instrument operating at 100.5 MHz with samples packed into a zirconium oxide rotor. The ^{13}C chemical shifts were calibrated indirectly through the adamantane peaks (δ = 38.3, 29.2) related to $SiMe_4$. Cyclic voltammograms were recorded at scan rates ranging between 50 and 1000 mV s^{-1}, using an EG&G Model 273 at 20 °C in a Metrohm voltammetric cell, with a combined working and counter platinum electrode and a standard Ag/AgCl (in KCl 3.5 M; 0.2050 V) reference electrode. Aldrich anhydrous methylene chloride was used as a solvent (sample concentration about 1 × 10^{-4} M), and tetrabutylammonium tetrafluoroborate (TBAFA) as a supporting electrolyte (5 × 10^{-2} M). Reported data are referred to the F_c^+/F_c reversible couple (F_c = ferrocene; $E_{1/2}$ = 0.6425 V vs Ag/AgCl 3.5 M).

Disubstituted Imidazolidine-2-thione-4,5-thiones (4a−j). These products were prepared according to literature methods[52] by reacting an appropriate *N*,*N*′-dialkylthiourea or *N*-alkyl-*N*′-arylthiourea[53] with oxalyl chloride in CH_2Cl_2 solution and were recrystallized from CH_2Cl_2 or ethyl ether.

[Ni(R,R′timdt)$_2$] (7a−i). As previously pointed out,[15,16] both nickel powder and nickel chloride can be used in these syntheses, although much better results are obtained starting from the metal as powder. A general synthesis consists of refluxing about 5 mmol of the disubstituted imidazolidine-2-thione-4,5-thione (**4a−j**) with a slight excess (about 10%) of Lawesson's reagent[22] (**5**) in 100 mL of previously degassed toluene for a time varying between 20 min and 1 h, depending on the substituents. After concentration of the reaction mixture, EtOH was added to lower the solubility of the complex and the dithiolene was filtered off. From the remaining solution, the 4,5,6,7-tetrathiocino[1,2-*b*:3,4-*b*′]diimidazolyl-1,10-dialkyl$_1$-3,8-dialkyl$_2$-2,9-dithione derivatives[20] and *trans*-bis[*O*-ethyl(4-methoxyphenyl)phosphonodithioato]-Ni(II) were generally isolated.[29,54] The yields in dithiolene strongly depend on the substituents, vary between 5% (**7a**) and 55% (**7e**), and are always low with aromatic substituents (**7j** was never obtained). Nickel-dithiolenes are recrystallized from chloroform/ethyl alcohol mixtures. Among all attempts to obtain crystals suitable for X-ray structural determination, only crystals of **7c** were grown from a 5:1 toluene/hexane mixture. Elemental analyses correspond to expected values. Ni-dithiolenes decompose in a range between 200 (**7f**) and 270 °C (**4a−c**).

[Pd(R,R′timdt)$_2$] (8a−j). Compounds **8a−j** were synthesized according to the procedure previously described for **8b**,[18] starting from compounds **4**. Also in these cases, compounds **6** and **10** were obtained as byproducts.

[Pt(R,R′timdt)$_2$] (9a−j). Starting from $PtCl_2$, the syntheses of **9a−j** are very similar to those for Pd analogues. Unlike the case of Ni and Pd, no Pt-phosphonodithioate complex was isolated as a byproduct.

X-ray Crystallography. Crystal data for **7c**: $C_{14}H_{20}N_4NiS_6$, fw 495.54, triclinic, space group *P*-1 (no.2), a = 5.723(3) Å, b = 9.580(6) Å, c = 9.670(6) Å, α = 97.79(2)°, β = 104.12(2)°, γ = 91.26(2)°, V = 508.6(5) Å^3, Z = 1, D_{calc} = 1.620 g cm^{-3}, μ (Mo−Kα) = 15.6 cm^{-1}. 2007 reflections were collected at room temperature on an Enraf-Nonius CAD4 diffractometer, with graphite-monochromatized Mo Kα radiation (λ = 0.71073 Å) in the 3−25° θ range. The intensities were

(52) Stoffel, P. J. *J. Org. Chem.* **1964**, *29*, 2794.
(53) Hecht, O. *Ber.* **1890**, *23*, 281.
(54) Although ethyl alcohol was used for the mentioned syntheses, analogous results were obtained in methyl alcohol.

corrected for Lorentz-polarization and absorption effects.[55] The structure was solved by Patterson and Fourier methods and refined with full-matrix least-squares, assigning anisotropic displacement parameters to all the non-hydrogen atoms. $R = 0.043$, $R_w = 0.048$ for 1122 observed reflections having $I > 3\sigma(I)$.

Crystal data for **6a**: $C_{22}H_{20}N_4S_6$, fw 532.82, monoclinic, space group $C2/c$ (no. 15), $a = 15.419(2)$ Å, $b = 15.799(2)$ Å, $c = 12.989(1)$ Å, $\beta = 126.14(1)°$, $V = 2555.3(6)$ Å^3, $Z = 4$, $D_{calc} = 1.385$ g cm^{-3}, μ (Mo Kα) = 5.3 cm^{-1}. 14073 reflections in the 0−26° θ range were collected at room temperature on a Siemens SMART CCD diffractometer, with graphite-monochromatized Mo Kα radiation ($\lambda = 0.71073$ Å). The intensities were corrected for Lorentz-polarization and absorption effects (SADABS)[56] and merged giving 2944 unique reflections ($R_{int} = 0.023$). The structure was solved by direct methods (SIR97)[57] and refined with full-matrix least-squares, assigning anisotropic displacement parameters to all the non-hydrogen atoms. $R = 0.026$, $R_w = 0.033$ for 1986 observed reflections having $I > 3\sigma(I)$.

For both structures scattering factors were taken from Cromer and Waber.[58] Anomalous dispersion effects were included in F_o; the values for $\delta f'$ and $\delta f''$ were those of Cromer.[59] All calculations were performed using Personal SDP software.

Computations. Quantum chemical calculations were carried out using the commercially available suite of programs Gaussian 94 and 94W.[60] Density functional calculations[61] (DFT) were performed using the hybrid Becke3LYP functional (which uses a mixture[62] of Hartree−Fock and DFT exchange along with DFT correlation: the Lee−Yang−Parr correlation functional[63] together with the Becke's gradient correction).[64] The basis set for all calculations was the Schafer, Horn, and Ahlrichs pVDZ basis[65] for C, H, N, and S, while for Ni, Pd,and Pt, we used the Hay-Wadt LANL2DZ basis sets together with ECP sets.[36] Numerical integration was performed using the FineGrid option, which indicates that for each atom a total of 7500 points are used. After a geometry optimization performed starting from structural data regularized in order to satisfy the D_{2h} symmetry, harmonic frequencies were obtained by diagonalization of the second derivatives of the DFT energy, computed by numerical differenziation of the DFT energy gradients.

Acknowledgment. This project was carried out as part of the "Progetto Finalizzato Materiali Speciali per Tecnologie Avanzate II" of the "Consiglio Nazionale delle Ricerche". We acknowledge Dr. Greta De Filippo for her contribution to the synthesis of some compounds. We also wish to acknowledge the Regione Basilicata for a contribution to the development of the Laboratorio di Sintesi e Caratterizzazione di Materiali Innovativi (LaMI).

Supporting Information Available: Tables giving details of the data collection and refinement, atomic coordinates, displacement parameters, bond lengths and angles. Optimized geometries in Cartesian coordinate form and frontier Kohn−Sham orbital energies at the Becke3LYP level for compounds **1**−**3**, **11**−**13**, and **14**−**16**. Elemental analyses, melting points, solid-state FT-IR and FT-Raman, UV−vis−NIR, and CP-MAS ^{13}C NMR spectra for each prepared compound are available on request. This material is available free of charge via the Internet at http://pubs.acs.org.

JA990827X

(55) North, A. C.; Phillips, D. C.; Mathews, F. S. *Acta Crystallogr.* **1968**, *A24*, 351.

(56) Sheldrick, G. M. SADABS, University of Gottingen, Germany, 1996, to be published.

(57) Altomare, A.; Cascarano, G.; Giacovazzo, C.; Guagliardi, A.; Burla, M. C.; Polidori, G.; Camalli, M. *J. Appl. Crystallogr.* **1994**, *24*, 435.

(58) Cromer, D. T.; Waber, J. T. *International Tables for X-ray Crystallography*; The Kynoch Press: Birmingham, England, 1974; Vol. IV, Table 2.2B.

(59) Cromer, D. T.; Waber, J. T. *International Tables for X-ray Crystallography*; The Kynoch Press: Birmingham, England, 1974; Vol. IV, Table 2.3.1.

(60) Gaussian 94 (Revision D.1 & E.1): Frisch, M. J.; Trucks, G. W.; Schlegel, H. B.; Gill, P. M. W.; Johnson, B. G.; Robb, M. A.; Cheeseman, J. R.; Keith, T. A.; Petersson, G. A.; Montgomery, J. A.; Raghavachari, K.; Al-Laham, M. A.; Zakrzewski, V. G.; Ortiz, J. V.; Foresman, J. B.; Peng, C. Y.; Ayala, P. Y.; Wong, M. W.; Andres, J. L.; Replogle, E. S.; Gomperts, R.; Martin, R. L.; Fox, D. J.; Binkley, J. S.; Defrees, D. J.; Baker, J.; Stewart, J. P.; Head-Gordon, M.; Gonzalez, C.; Pople, J. A. Gaussian, Inc., Pittsburgh, PA, 1995.

(61) (a) Labanowsky, J.; Andzelm, J. *Density Functional Methods in Chemistry*; Springer-Verlag: New York, 1991. (b) Ziegler, T. *Chem. Rev.* **1991**, *91*, 651 and references cited therein. (c) Scheiner, A. C.; Baker, J.; Andzelm, J. W. *J. Comput. Chem.* **1997**, *18*, 775.

(62) Becke, A. D. *J. Chem. Phys.* **1993**, *98*, 1372.

(63) Becke, A. D. *J. Chem. Phys* **1993**, *98*, 5648.

(64) Lee, C.; Yang, W.; Parr, R. G. *Phys. Rev. B* **1988**, *37*, 785.

(65) Schafer, A.; Horn, H.; Ahlrichs, R. *J. Chem. Phys.* **1992**, *97*, 2571.